A Hybrid Heavy-Duty Diesel Power System for Off-Road Applications – Concept Definition

Chad Koci, Jay Steffen, Rich Kruiswyk, Fang Guo, Tim Bazyn, and Robert McDavid
Caterpillar Inc.

Radoslav Ivanov
R-Flow Ltd.

Dheeraj Sirimalla
Volt Management Corp.

Abstract

A multi-year Power System R&D project was initiated with the objective of developing an off-road hybrid heavy-duty concept diesel engine with front end accessory drive-integrated energy storage. This off-road hybrid engine system is expected to deliver 15 – 20% reduction in fuel consumption over current Tier 4 Final-based diesel engines and consists of a downsized heavy-duty diesel engine containing advanced combustion technologies, capable of elevated peak cylinder pressures and thermal efficiencies, exhaust waste heat recovery via SuperTurbo™ turbocompounding, and hybrid energy recovery through both mechanical (high speed flywheel) and electrical systems. The first year of this project focused on the definition of the hybrid elements using extensive dynamic system simulation over transient work cycles, with hybrid supervisory controls development focusing on energy recovery and transient load assist, in Caterpillar's DYNASTY™ software environment. Three key off-road applications were the focus of the hybrid concept definition with an aim of understanding the system's modular capability for the diverse off-road heavy-duty market. Core engine performance 1D and 3D simulations isolated the efficiency contributions from the downsized engine, turbocompounding, and in-cylinder thermal barrier coatings. A fuel consumption improvement range of 14 to 24% was predicted, resulting in successful project progression to the design and experimental validation phase. An overview of the experimental engine and hybrid system status concludes the discussion along with the multi-year project's next steps.

Introduction

Driven by the need for sustainability and economic value, the heavy-duty off-road industry greatly values R&D towards increases in fuel efficiency. Total cost of ownership (TCO) is a primary metric for heavy-duty products, and the off-road sector is no exception. Fuel consumption can be a large factor and even the dominant factor when calculating the TCO for a given off-road product. Decreases in fuel consumption can therefore justify financial investment and acceptable payback periods, if significant enough in magnitude. Sustainability may also be as strong, or stronger of a driver for reduced fuel consumption, and efficiency improvements at the off-road machine/product level may be required to meet site-level metrics, such as allowable greenhouse gas (GHG) emissions. Caterpillar has a long history of addressing efficiency and fuel consumption with a first level of powertrain and machine technologies, centered on optimizing and right-sizing the system. Examples of this are the hydraulic-hybrid excavators, which were introduced in 2012 [1], and the following electric-drive dozers [2,3] and large wheel loaders[4].

Continuing to be motivated by these economic and sustainability forces, the present ongoing project aims to research and develop additional and differentiated technologies applicable for off-road Power Systems which could make a significant efficiency impact. The performance targets for this project are:

- 17 (+/-2) % more fuel efficient than current Tier 4 diesel engine
- Equivalent transient response vs. baseline diesel engine
- Tier 4-Final exhaust emissions levels

If these performance targets can be achieved, the proposed improvements applied to Caterpillar's off-road product range would save more than twenty-five million barrels of oil over ten years. And this would then deliver the critical sustainability and TCO improvements required.

This multi-year powertrain R&D project was awarded by the U.S. Department of Energy, Office of Energy Efficiency and Renewable Energy in the 2018 funding opportunity announcement DE-FOA-0001919. Following this award and funding announcement, multiple other Department of Energy R&D off-road funding announcements and awards were granted. The University of Wisconsin-Madison with their project entitled "Improving Efficiency of Off-Road Vehicles by Novel Integration of Electric Machines and Advanced Combustion

Engines" looks to be pursuing a hybrid electrification pathway coupled with some amount of an advanced combustion system [5]. A similarly entitled project "Improved Efficiency of Off-Road Material Handling Equipment through Electrification" from Michigan Technical University also seems to be focusing on how to use electrification to improve off-road efficiency [6]. Clearly there is a recent surge of need and interest toward the goal of improving off-road equipment and product efficiency.

The focus over the past ten years, not surprisingly based on quantity of energy consumption, has generally been on the on-road or on-highway heavy-duty sector with the SuperTruck and SuperTruck II Department of Energy programs. Looking toward these programs it can be seen how there is a universal adoption of some amount of Power System and powertrain hybridization. The Cummins-Peterbuilt SuperTruck II project is using a 48V mild hybrid system with electric cooling fans and a Motor Generator Unit (MGU) integrated on the transmission [7]. A 48V mild hybrid system from Daimler [8] incorporates electrified pumps, fans, engine starter and a P2 position for the MGU. 48V mild hybrid systems from both PACAAR [9] and Volvo [10] also involve electrified fans, pumps, and parasitic elements which were traditionally mechanically driven. Navistar looks to have the only SuperTruck II project not using solely a 48V electric-hybrid system, as they are carrying along in parallel a high voltage system [11]. The vehicle system optimization nature of the SuperTruck II program allows for all the power and energy devices to be consolidated into a common electrical system, if a system of sufficient power is present, which is very logical. From the SuperTruck II available documentation the electric-hybrid MGU power limits seem to be near ~30kW (for the 48V systems). This power level is perceived to be low when considering off-road applications with their more severe duty cycles, machine implement loadings, and transient load response requirements. Using the SuperTruck II hybrid system efforts as a backdrop, the differences in the hybrid system technologies for off-road applications will be interesting to compare and contrast.

The result of the R&D effort will be the design of a high-efficiency Power System with a 13L concept engine – downsized from 18L – for use in off-road machine applications. The 18L to 13L downsizing was selected due to a wide application opportunity and for understanding of how hybridization may help with this difficult ~30% downsizing magnitude. The Power System will have hybrid elements and a front-end accessory drive (FEAD) that incorporates:

- High-Speed Flywheel (HSFW)
- Mechanical-drive Turbocharger (SuperTurbo)
- Motor-Generator Unit (MGU)

The project will culminate in a physical demonstration of the high-efficiency Power System. The demonstration will occur in a high-capability test cell with the engine, all the hybrid devices, controls, and required performance and emissions measurements.

Power System vs. Powertrain Paradigm

A unique aspect of off-road applications and this project is the idea of a Power System as opposed to a powertrain. Figure 1 attempts to draw the boundary diagram demarking the difference between a powertrain and a Power System. A Power System is unique because it delivers power to some boundary condition, like the flywheel-transmission interface, which is not the final destination for useful work. The hybrid elements of this program are contained within the Power System boundary, while the resulting off-road machine performance is outside of the boundary. Therefore, the goal of the Power System is to match the current machine performance with increased efficiency without knowledge or alteration to the upper machine system level.

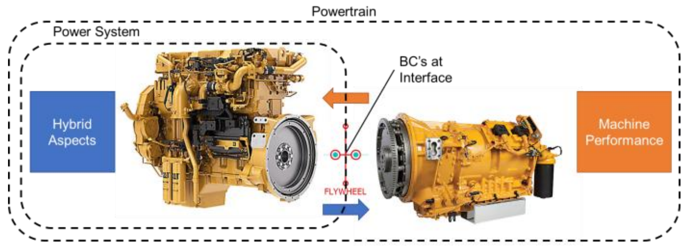

Figure 1. Boundary diagram illustrating the difference between a powertrain and a Power System.

Figure 2 is a brief example of why the concept of a Power System without knowledge or alteration to the upper machine level is important. The off-road market is highly diverse, and the 29 machine applications shown illustrate just the powertrain diversity of the first-fit applications; the landscape gets even further diverse and complicated when considering third-party applications. Accompanying the application and powertrain diversity is a lack of unit volume. Many heavy-duty off-road machines, specifically larger machines, are on the order of hundreds or thousands as opposed to tens of thousands or hundreds of thousands for on-road. A modular and efficient hybrid Power System paradigm is required to overcome the otherwise insurmountable R&D effort.

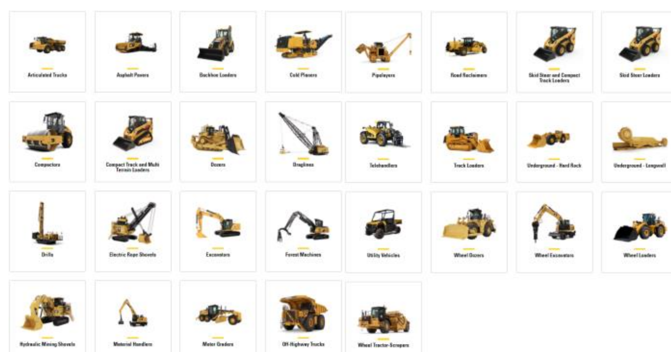

Figure 2. An illustration of 29 of the highly diverse off-road machine applications; all applications have unique power, energy, and efficiency requirements.

Three Key Machine Applications

The three key off-road machine application selected for this R&D project were the 988K large wheel loader (LWL), the 390F hydraulic excavator (HEX), and the 745 articulated truck (AT), Figure 3. These represent some of the major off-road construction machine types, each with different powertrains, uses, needs, and constraints.

Figure 3. The three key machine applications selected for the baseline. All three are powered today by a Cat® C18 ACERT™ diesel engine.

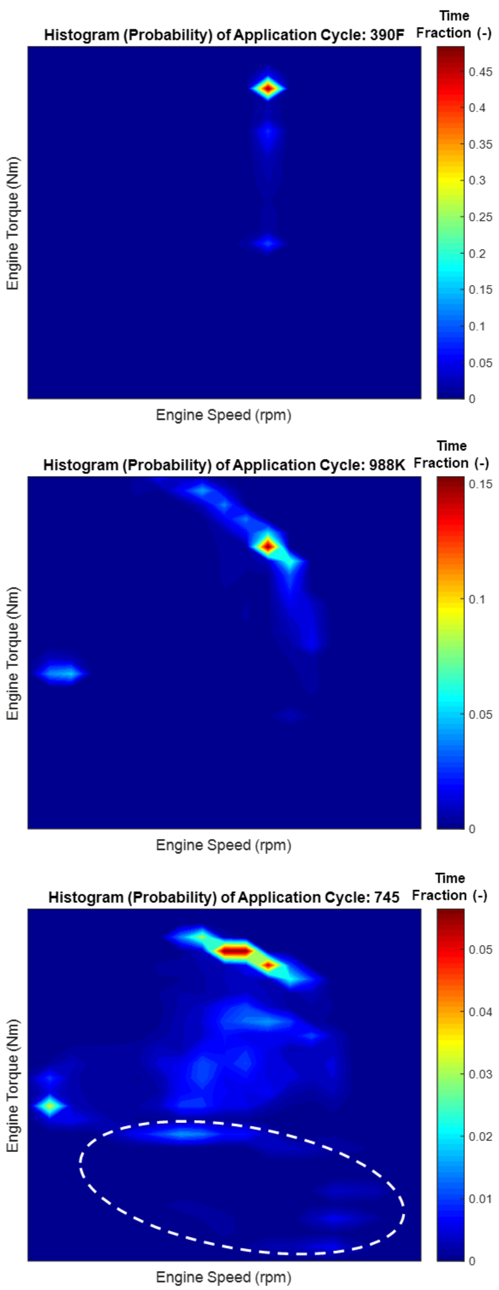

Figure 4. Representative work cycle engine speed/torque 2D histograms showing where operation occurs. The white circle is where brake energy recovery is possible.

In Figure 4 the representative work cycle engine speed/torque 2D histograms highlight where each of the three key machine applications operate. A common theme is one of high load and high power, which is not unexpected from heavy-duty equipment. The powertrains produce different operation histograms and only one application, the 745AT, has recoverable energy at the Power System boundary. This is from the existing engine compression release brake used to retard the truck. The data and transient work cycles behind these histograms are the target for the hybrid concept simulations and definition.

These histograms do not include significant engine idle periods which do exist in real applications. A detailed start/stop analysis will not be reviewed in this paper, but anywhere from 2-4% fuel consumption reduction can be found in these three key applications with reasonable assumptions regarding machine accessory energy and starting system capability.

At present all three of the Tier 4 Final key off-road machines are powered by a Cat C18. The developed hybrid Power System will shift to the aforementioned concept 13L engine, which represents a significant (and difficult) 30% increase in power density.

Figure 5. Significant 30% engine downsizing to replace the key machine Cat C18 ACERT diesel engine Power System.

Hybrid Concept Layouts & Functionality

The approach and core functionality of the hybrid concept is to add hybrid power and energy elements to enable:

- Engine Downsizing
    - Transient load assist to maintain machine productivity
- Energy Recovery
- Start/Stop (or Anti-Idle)

The initial proposal involved the integration of the FEAD, a HSFW, and turbocharger onto the front of the engine. As shown in Figure 6 below, the turbocharger was coupled to the HSFW to allow direct energy transfer. Also, the system could be de-clutched from the engine for stop-start functionality and energy transfer from the HSFW to the FEAD. An MGU was also proposed as an alternator replacement on the FEAD.

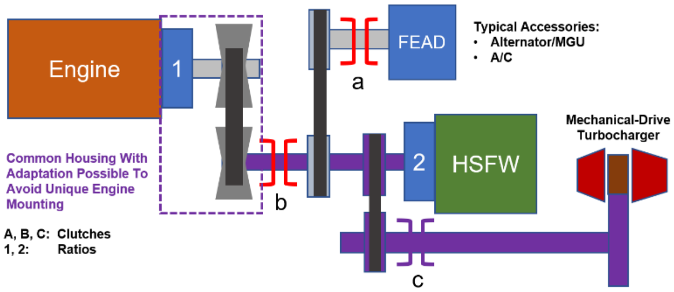

Figure 6. The initial off-road hybrid Power System concept.

Initial simulations, research into available technologies, and packaging studies led to the creation of three main concepts involving different ways to integrate the turbocharger, which in this case was a SuperTurbo from SuperTurbo Technologies.

Concept 1 (Figure 7) connected the SuperTurbo CVT directly to the HSFW similar to the initially proposed concept. The HSFW was then coupled to the engine via a clutch, belt-type CVT and engine disconnect clutch. The FEAD and MGU were coupled to the belt-type CVT to allow energy transfer between the HSFW and FEAD with the engine disconnected and not running.

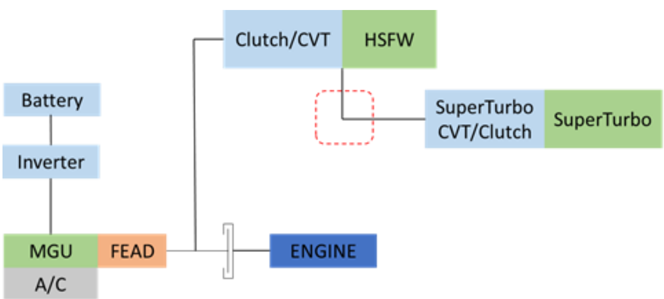

Figure 7. Hybrid Power System concept 1.

Concept 2 (Figure 8) kept the FEAD and HSFW connections to the engine the same as Concept 1 but independently connected the SuperTurbo to the engine crankshaft instead of going through the HSFW.

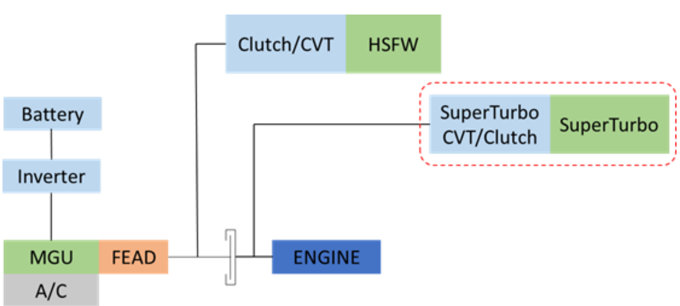

Figure 8. Hybrid Power System concept 2.

Concept 3 (Figure 9) also kept the FEAD and HSFW connections to the engine the same as Concept 1 but instead of mechanically connecting the SuperTurbo to the engine, the SuperTurbo was driven by an additional MGU. This MGU was placed on the same DC bus as the FEAD MGU.

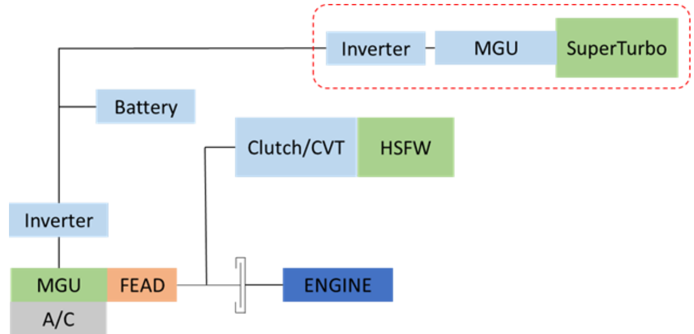

Figure 9. Hybrid Power System concept 3.

Concept down-selection involved creating plant and controller models for each concept and simulating machine application cycles using system simulation in DYNASTY. The cycle results were analyzed for efficiency, response, and controllability. The concepts were mocked-up in 3D CAD software (CREO®) to evaluate the packaging with respect to the new concept engine. Also, the system concepts were evaluated based on maturity of the technology and feasibility of the concept being able to demonstrate the program targets within budget and time schedules.

Concept 1 (Figure 7) was eliminated based on several deficiencies uncovered. Packaging was a major concern as both components had to be coupled on the same side of the engine and had interference with major engine components. It was also found the combined ratio range of both the HSFW CVT and SuperTurbo CVT were not wide enough to cover the desired turbo speed ranges for maximum efficiency. Reduced turbocompounding efficiency was also a drawback to this concept as when recovering excess energy from the turbocharger, additional energy would be lost going through the HSFW CVT. This concept would be more efficient if the excess energy was stored in the HSFW, but it was found that the most efficient use was to return the energy back to the crankshaft to reduce engine fuel consumption. These reasons, as well as additional controls complexity of having the SuperTurbo and HSFW system coupled, eliminated the concept from consideration.

Concept 3 (Figure 9) was next to be eliminated, although on an efficiency basis it was found to be similar to Concept 2. Possible advantages over Concept 2 were identified including packaging and response rate but were outweighed by the technical challenges of the integration of the MGU into the SuperTurbo, as well as increased controls complexity. Future usage of the SuperTurbo technology was also considered as it may be used without a 48V system available, so more benefit was seen with integrating it mechanically.

Concept 2 (Figure 8) was selected; plant model and controller updates were made, and many hours of simulation were performed to further characterize the performance. During this time deficiencies were found in the HSFW system. The ratio response of the HSFW belt CVT transmission was not fast enough to track the high engine acceleration rates and thus caused un-commanded loads on the Power System. The transient response and assist requirements of the Power System could not be met due to the combination of the reduced response rate and power transmission capability of the CVT. This led to the exploration of alternative HSFW transmission systems.

The main alternative transmissions evaluated were a multi-speed gearbox with clutches, a hydrostatic variant, and an electric drive. The multi-speed gearbox (Figure 10) was eliminated as a concept due to abundance of new project content as well as estimated lower efficiency. The hydrostatic option (Figure 11) was developed with expected component sizing and built into a simulation model with controls. The simulations showed the concept was feasible and could use an off-the-shelf hydraulic pump and motor. The response rate was much faster than the belt CVT but the system still suffered from having the HSFW ratio-coupled to the engine and thus was affected by high engine acceleration. The hydrostatic transmission option is worth further study for future programs but was eliminated as a concept for this project. The electric drive concept (Figure 12) was selected mainly due to having the best response rate of all options, as well as complete decoupling of the engine speed and flywheel speed. The ratio range constraint of other CVT's was also eliminated by the electric drive selection. In addition to the performance benefits, the packaging aspect was also improved since the HSFW would only need to be coupled to the engine with wiring and thus could be moved to available space around the engine and or machine installation.

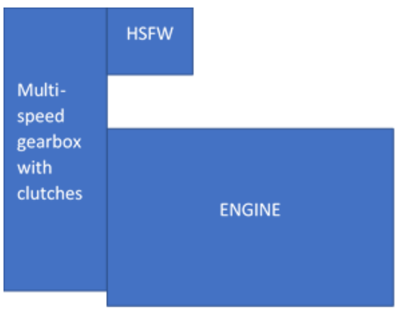

Figure 10. Multi-speed gearbox concept

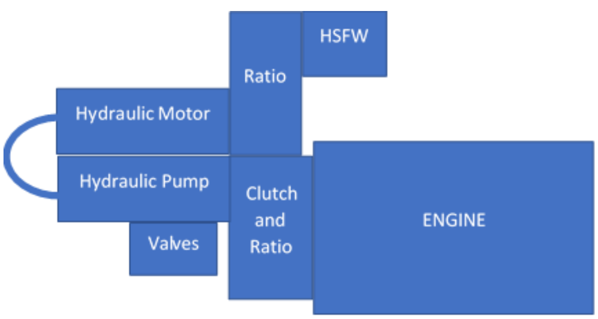

Figure 11. Hydrostatic transmission concept

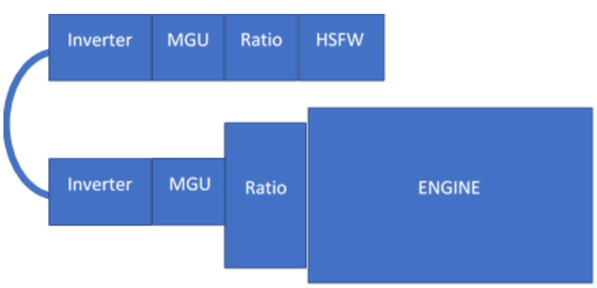

Figure 12. Electric-drive transmission concept

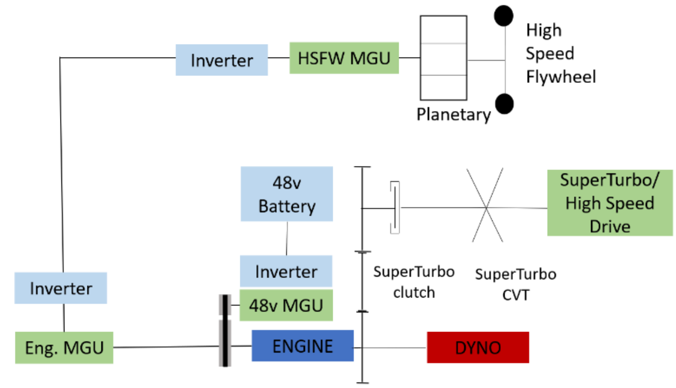

Figure 13. Concept 2a

The final transmission concept was integrated into the selected Concept 2, now named 2a, and is shown in Figure 13. It should be noted that a Concept 3a is compared later which is the same as Concept 3 in Figure 9, but with the same HSFW electric-drive of Concept 2a and Figure 12. The Concept 2a includes the HSFW driven by an electric drive transmission, 48V MGU, and SuperTurbo all having independent connections to the engine crankshaft. Due to packaging concerns and multiple other connections with the front of the engine, the SuperTurbo connection was moved to the rear PTO of the engine instead of the FEAD.

Hybrid System Transient Simulations

In order to evaluate the concepts described in the previous section, a high-fidelity transient Power System model was developed in DYNASTY. DYNASTY [12-14] is Caterpillar's multi-domain system simulation software which is widely used throughout the enterprise as it enables the virtual integration of many different subsystems, including Engines, Aftertreatment, Hydraulics, Driveline, Electrical Machines, Cooling, Electronics and Controls, etc.

Model Setup & Structure

In order to meet the needs of the project, the Power System model required the modelling and integration of the following subsystems:

Plant subsystems:

- Engine
- Dyno
- SuperTurbo
- High Speed Flywheel (HSFW)
- Motor Generator Unit (MGU)
- Battery

Controller subsystems:

- Engine Controller
- Dyno Controller
- SuperTurbo Controller
- High Speed Flywheel (HSFW) Controller
- Motor Generator Unit (MGU) Controller
- Battery Management System
- L5 Supervisory Controller

In addition, each of the subsystems listed above have multiple implementations representing different hardware configurations, different levels of fidelity and different software iterations.

In order to keep the modelling effort consistent and focused throughout the project, the team chose to use a single Power System model which can be configured to represent any of the Hybrid Concepts discussed earlier. In addition, each concept can be configured with different implementations for each subsystem, depending on the simulation task being performed. For example, fast-running Engine plant implementations can be loaded by the Controls team in order to aid the controls development velocity. Another example would be to configure the Power System model to represent the C18 baseline by selecting a C18 engine implementation and disabling all the hybrid devices. This approach enables fair and robust back-to-back performance comparisons between the new concepts and the baseline.

Figure 14 illustrates the top-level view of the DYNASTY Power System model.

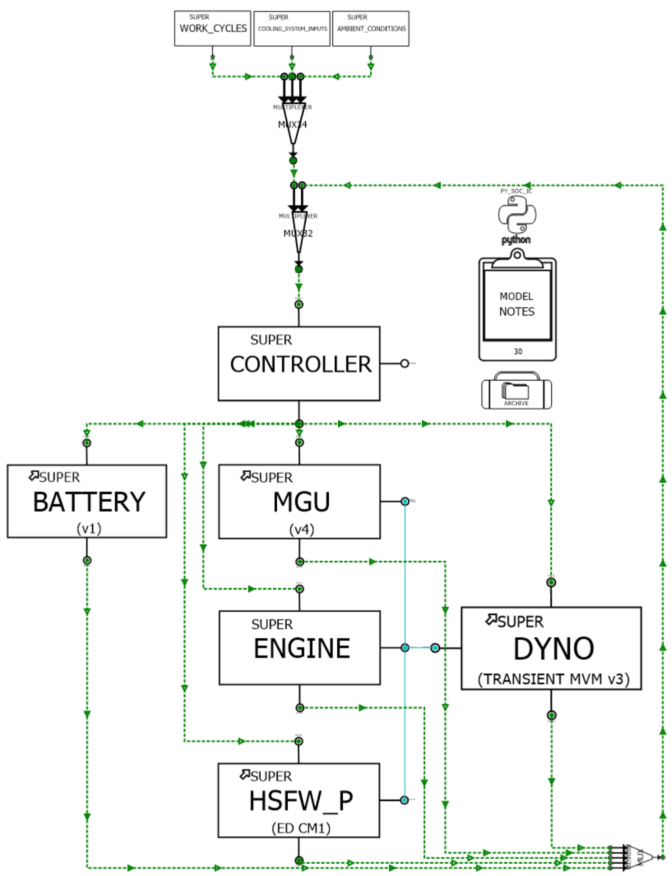

Figure 14. DYNASTY Power System Model – top-level view

Full cycle results

In order to evaluate the performance of the different concepts for the three key machine applications (745 articulated truck (AT), 390F hydraulic excavator (HEX) and 988K large wheel loader (LWL)), a total of 19 representative work cycles were identified and made available for simulation in the DYNASTY Power System model. The total length of the down-selected cycles is over 5 hours real time. Each individual cycle is based on real-world data collected on different customer machines operating in the field. The off-highway / heavy-duty applications are much more diverse and even the same machine can be subjected to very different operating conditions depending on customer's site location, characteristics and productivity targets.

In addition, the DYNASTY Power System model has been used extensively not only for the Hybrid Concept down-selection, but also for L5 supervisory controller strategy down-selection and battery sizing. Using a high-fidelity Power System model for transient simulations of long machine cycles makes the local model execution impractical. Therefore, most of the simulation runs had to be executed on a High-Performance Computing (HPC) cluster.

Figure 15 illustrates the performance differences between concepts 2a and 3a relative to the C18 baseline performance. All the results shown are DYNASTY Power System Model predictions and the positive values indicate that Concepts 2a and 3a demonstrate better efficiency when compared to the C18 baseline.

When summarizing the results by application (top bar chart) it is evident that the 745 articulated truck (AT) application cycles (1-9 in Figure 15) are more favorable when it comes to efficiency improvement opportunities. Those cycles comprise of relatively steady-state operating conditions which enable good turbo-compounding gains. In addition, by using the MGU and to a lesser extent – the HSFW during portions of the cycles where retarding is required, additional energy can be recovered and stored in the battery instead of being transformed into heat and lost to the environment when using the engine compression release brake. This recovered and stored energy can be used later during the cycle to offset some of the engine fuel energy depending on the L5 supervisory logic.

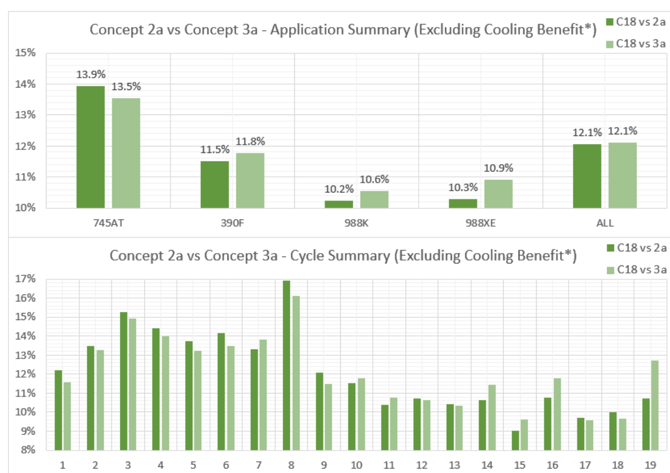

Figure 15. DYNASTY Power System Simulation Results – predicted efficiency benefit of concepts 2a and 3a vs the C18 baseline
** The Cooling Benefit is discussed in more detail the Heat Rejection and Thermal Barrier Coatings section of this paper*

The 390F hydraulic excavator (HEX) and 988K large wheel loader (LWL) cycles (10-19 in Figure 15) are much more transient by nature. They are characterized by frequent transitions in engine operating conditions from relatively low load to high/rated load (Figure 4) with almost no recoverable energy available at the Power System boundary (Figure 1). This reduces the predicted benefit not only because almost no energy can be recovered and stored in the battery during those cycles, but also because the HSFW, MGU and SuperTurbo need to assist the engine during a significantly increased number of transient events. Under those circumstances the energy required to power the additional hybrid devices is drawn mainly from the engine crank, thereby reducing the efficiency improvement over the C18 baseline.

When it comes to the relative performance of Concept 2a versus Concept 3a, the differences are very slim, irrespective of the application cycle. This indicates that both the mechanically driven SuperTurbo (Concept 2a) and the alternative electrically driven SuperTurbo (Concept 3a) options demonstrated very comparable efficiencies. In addition, the perceived advantage of Concept 3a to be able to store the recovered energy in the battery as opposed to using it immediately to offset engine fuel did not impact the efficiency improvement predictions with the exception of a few 988K large wheel loader (LWL) cycles (14, 16 and 19 in Figure 15).

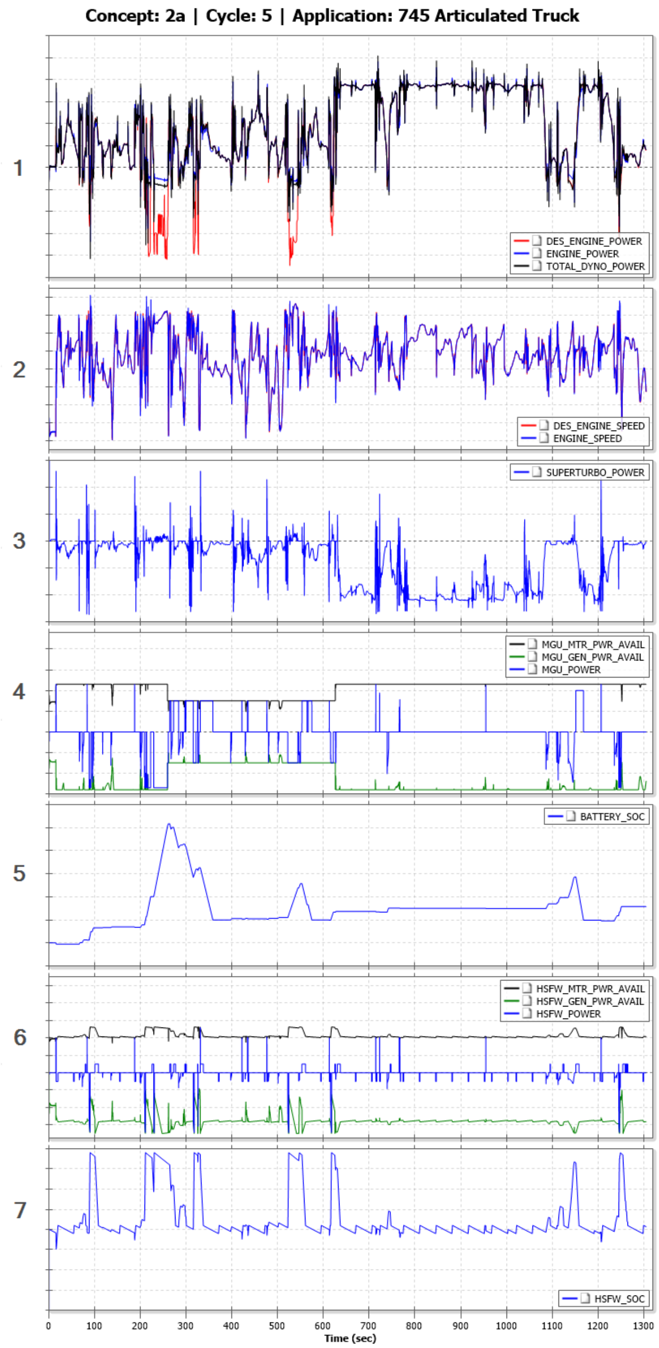

Figure 16. DYNASTY Power System Simulation Results – Concept 2a, Cycle 5, 745 Articulated Truck application Note: Hybrid Device Power signs: positive = assist; negative = regen

Ultimately the decision to proceed with Concept 2a instead of Concept 3a was based on considerations discussed in the Hybrid Concept Layouts & Functionality section of this paper as performance-wise the two concepts were very close to one another.

In order to better illustrate the interactions between the different hybrid devices and the engine, Figure 16 presents timeseries simulation results of Concept 2a simulated over 745 articulated truck (AT) application cycle 5.

Cycle 5 is based on real-world customer data with a length of just over 1300 seconds and demonstrates some typical articulated truck cycle features: relatively steady-state operating conditions (Figure 16, 625s-1025s) combined with portions where extra retarding power from the engine compression release brake equipped C18 is available for recovery (Figure 16, 200s-270s, 320s-350s, 530s-550s, 640s-650s).

The simulated 2a Power System concept targets the same power/torque and engine speed as the compression release brake equipped C18 baseline (Figure 16, plots 1 and 2). Where the negative power of the C18 baseline (DES_ENGINE_POWER) is lower than the 13L engine motoring curve, additional energy can be recovered by the MGU and HSFW devices when they are switched into regen mode.

The SuperTurbo is tasked with assisting the engine during acceleration events by providing additional power to the turbo shaft (Figure 16, plot 3). This results in increased turbo speed, boost pressure and consecutively – AFR limit, allowing more fuel to be injected during the transient event. In addition, during prolonged operation at high load conditions (Figure 16, 625s-1025s), the SuperTurbo harvests the extra energy from the exhaust gasses which would have otherwise been lost due to wastegate operation during those operating conditions.

The MGU and the Battery are two of the devices in the Power System which enable the recovery, storage and reuse of the recoverable energy available (Figure 16, plots 4 and 5). Since the Battery has much greater storage capacity than the HSFW, it stores most of the recoverable energy. It also enables the MGU to assist the engine when the L5 controller decides to convert some of the energy stored in the battery into MGU assist power, thus reducing the engine fueling. The MGU itself also has a secondary task of assisting the SuperTurbo during transient events. Since the power ratings of the MGU and SuperTurbo are well matched, when there is a case of simultaneous assist event from the SuperTurbo and the MGU, no additional power is drawn from the engine crank and the energy stored in the battery is used instead.

Since many off-road applications undergo heavy and frequent transient events, the maximum power rating of the MGU/Battery constrained by the 48V architecture (~30kW) is often not sufficient to assist the engine during a sudden load increase. On the other hand, achieving higher electrical power levels by using higher power MGU and more importantly – larger capacity battery with sufficiently high C-rating would pose a significant challenge on the Power System approach from packaging and cost considerations. Under these circumstances the HSFW provides a good solution for off-road applications in combination with a 48V based MGU/Battery system.

The HSFW allows much higher assist and regen powers to be achieved compared to the 48V MGU. Even with the limited HSFW energy storage capacity compared to the battery, the HSFW is particularly suitable for transient assist events where the duration of those assist events is quite short, thus not requiring a lot of energy per assist event.

The HSFW operation is illustrated in Figure 16, plots 6 and 7. High power bursts can be observed during the frequent assist events throughout the cycle. In addition, the HSFW can also recover energy in addition to the MGU and store it as kinetic energy using the electric drive transmission (Figure 12). Once the HSFW has reached maximum state of charge (SOC), the HSFW Controller limits the available regen power.

The HSFW also has some distinguishing features when compared to the MGU/Battery combination. In Figure 16, plot 6 the reader can note that the maximum available assist and regen power (HSFW_MTR_PWR_AVAIL and HSFW_GEN_PWR_AVAIL) are a function of the HSFW SOC (Figure 16, plot 7). At higher HSFW SOC conditions the HSFW can reach higher assist and regen powers. In practice only the higher assist power can be realized as there is not much headroom for capturing extra energy using the HSFW when the HSFW SOC is almost at its maximum. Another HSFW specific feature is the fact that the HSFW loses charge over time due to friction losses in the flywheel mechanism. This necessitates the initiation of numerous micro-charge commands which keep the HSFW at a predefined minimum SOC level. It is desirable to set the minimum SOC level at the lowest possible setting in order to minimize the HSFW charge loss over time and reduce the frequency of the micro-charge commands. In practice the minimum SOC level is determined by the minimum HSFW assist power requirement for a typical transient event and can be adjusted as needed depending on the application.

The HSFW is best suited for transient cycles with frequent transitions in engine operating conditions (390F hydraulic excavator (HEX) and 988K large wheel loader (LWL)) as they lack prolonged steady-state operating conditions. Nevertheless, the HSFW is also helpful in most 745 articulated truck (AT) application cycles as its transient assist capabilities generally outweigh the energy lost to maintain the minimum SOC during the steady-state portions of the AT cycles.

Transient response results

Downsizing from an 18L engine to a 13L engine means that response metrics like transient response, block load capability and snap torque capability are crucial to maintain the productivity of the machine applications that are the focus of this project. During transients or block loads, the HSFW & MGU directly supplement power (gained & stored from braking & decelerations of machine applications) to the FEAD / engine crank, and the SuperTurbo drive (by taking in power from FEAD/ engine crank) spools up the turbo speed to boost the engine quickly. This combination helps the hybrid power system to achieve comparable response to the larger baseline engine. The mechanical aspect of turbocharger power draw from the crankshaft is in contrast to technologies such as electric turbocharger assist [15], where the energy is sourced differently and has different power, thermal, and timescale limitations.

Constant speed load acceptance (CSLA)

The Constant Speed Load Acceptance (CSLA) test / simulation assesses the load increase or block load capability of off-highway engines at constant speed. The test / simulation is done by holding the engine speed constant at 0 N-m torque initially, for some time, then suddenly increasing the throttle to 100% to make the engine reach peak torque at that speed. For a diesel engine with a turbocharger, this test evaluates the response performance capability of the engine, specifically 1) the ability to quickly reach peak torque / power and 2) the level of snap torque achievable (snap torque is the instant torque achievable before the fueling is limited by a fuel-air ratio controller – important to immediately support auxiliary load and machine load). In this project with a Hybrid Power System, CSLA test / simulation would also evaluate the capabilities of the HSFW, MGU, and SuperTurbo that are supporting the engine system during transients.

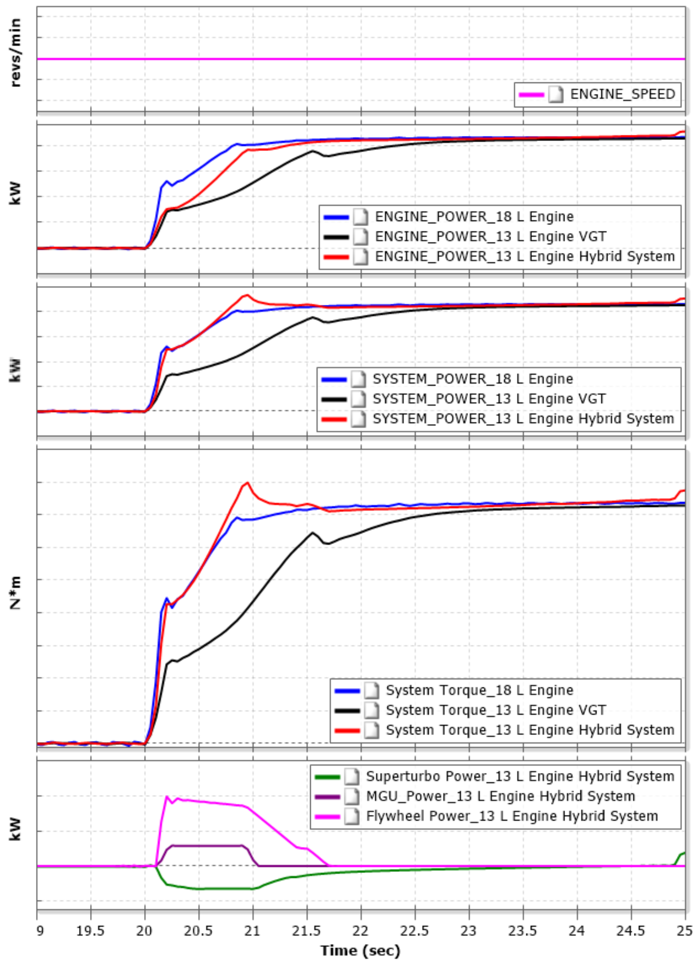

Figure 17 CSLA transient response comparison of C18 engine, 13L engine with VGT turbo & 13L engine hybrid Power System.

CSLA simulation results in Figure 17 compare the response of the 13L Engine / Hybrid Power System with the 13L Engine with variable geometry turbocharge (VGT) and with the baseline 18L Engine. The results in Figure 17 are for CSLA runs at 1400rpm, which is the peak torque speed for the 988K application, and is the highest torque level among the three applications. The plots in Figure 17 show that when a sudden load / throttle is imposed and the engine system is in transient mode, the Flywheel & MGU provide power to the FEAD and the SuperTurbo turbine is assisted from the FEAD / Engine crank

In Figure 17 plot 2 shows the engine power which represents the engine crankshaft location power of the C18 engine, 13L engine with VGT, and 13L engine with hybrid system. The system power in plot 3 of Figure 17 represents the total system power delivered at the dynamometer location. For the C18 engine and the 13L engine with VGT, the system power is same as the engine power whereas for the 13L engine with hybrid, the system power represents the sum of the engine and the additional device (HSFW, MGU, SuperTurbo) powers.

System level torque response comparison (fourth plot from the top in Figure 17) shows that snap torque and ensuing torque response of the 13L Engine Hybrid System matches the C18 engine torque. Plot 2 (second plot from the top in Figure 17) indicates the engine-only power transient response of the 13L Engine Hybrid System is improved compared to the 13L engine with VGT turbo, illustrating the SuperTurbo capability to enable better transient response by spooling the turbine faster and increasing the boost rate of the engine. Although the engine-only power of 13L Engine Hybrid System is lower than the C18 engine, the HSFW & MGU support the FEAD / PTO externally to get the system power/torque to match the C18 engine.

Torque Converter Stall Transient response (TC stall)

TC stall transient response simulations determine the engine's torque generating capability as it accelerates from low idle speed to stall speed at full throttle. Our simulation intent is to achieve acceptable off-idle transient engine acceleration against the load of the current torque converter used in the machine applications (988K, 745AT, 390F), which can be measured with the initial aforementioned "snap" torque, torque build rate, and speed ramp up as shown in Figure 19. The idea of torque converter stall test / simulation is to put the brakes on, go to full throttle, and have the torque converter absorb the load. TC stall test is modeled as shown below in Figure 18, where we have a torque converter, parasitic load of the machine, and a torque sink in the Dyno component of the full Power System model from Figure 14.

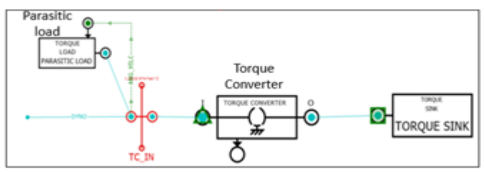

Figure 18. Model setup in DYNASTY for TC stall simulation.

Like the CSLA simulation, we have chosen 988K application for TC stall simulation as the 988K application peak torque requirement is higher compared to the other two applications. Simulation results in Figure 19 indicate both the stall speed of the engine and torque build response (including "snap" torque) of the 13L Engine Hybrid System is in-line or better than the C18 engine.

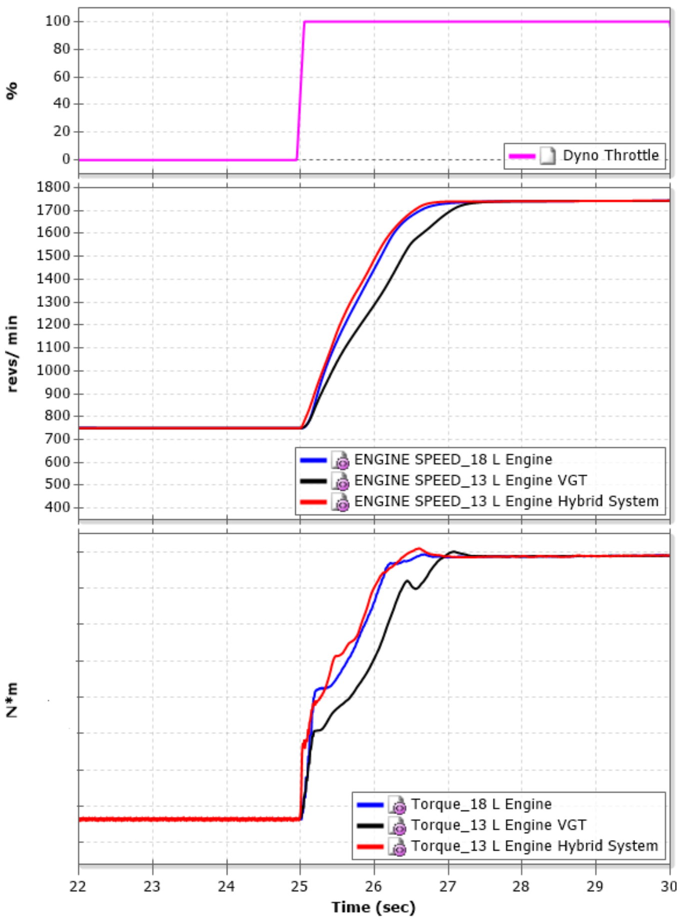

Figure 19. TC stall transient response comparison of C18 engine, 13L engine with VGT turbo & 13L engine hybrid Power System.

Hybrid Supervisory Controls

Power System Level Control Structure

The hybrid devices (MGU, HSFW, SuperTurbo) are designed to recover "free" energy and provide it back to offset fluid consumption during normal engine running. Exactly how to control or calibrate each device to minimize fluid consumption and meet the power request during transient events are the core functional requirements of the Power System level, designated as L5, controller. At each engine operating condition, the L5 controller categorizes the energy flow state based on the Machine level's (i.e. the Power System boundary condition) energy demand and Power System subcomponent/system level's, designated as L4, energy storage limit and availability. Then calculations are completed for the power request for each device at each state through closed loop proportional-integral-derivative (PID) controllers with the L4 devices, in order to either – (1) meet engine performance requirements (transient capability) or (2) maximize the recovery of energy (SuperTurbo turbocompounding, braking power); thus pushing to minimize fluid consumption (BSFC, TSFC). The fundamental building blocks for the L5 controller include a L4 health monitor, a L5 state vector, a L5 power request, and power limiting. The following sections discuss each control block in detail.

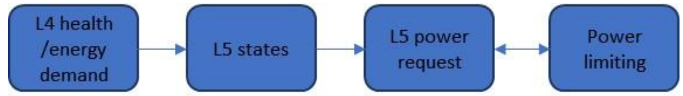

Figure 20. Power System (L5) supervisory controller structure.

L5 Controller Building Blocks

L4 Health Monitor / Machine Level Energy Demand

The L4 health monitor monitors L4 subsystem health conditions or energy states, and facilitates supervisory controller decision making regarding which L4 subsystems are available for energy flow path optimization, and/or which component needs to be supported with maintenance power from the other components. It also tracks the machine level energy demands: engine braking mode with recoverable energy, and engine acceleration state needing additional power assistance.

L5 States, Power Requests and Limiting

The information from the L5 health monitor / machine level energy demand is necessary to create two energy nodes: one that needs power, the other one that can provide power. The connection of these two nodes forms an energy flow path. A unique set of energy flow paths were defined based on the pre-determined feasible paths w.r.t the hybrid hardware concept configuration. The combination of any one or more energy flow paths were then explored and implemented in the control block of the L5 states through state flow modeling. This modeling covers four typical engine operation conditions: start, stop/braking, normal running, and acceleration. An example of the L5 states are listed in the rows of Table 1, where the SuperTurbo could provide turbo compounding power to Engine (row 1), or where the Engine provides shaft power to SuperTurbo to maintain optimal air fuel ratio (row 2), the HSFW and MGU both provide power with combined total value equivalent to what SuperTurbo needs during transient event (row 3), or harvest what is available as free energy during a braking event (row 4). The power split ratio "r" between the HSFW and MGU is optimized considering each devices respective L5 energy level constraint set.

Table 1. Example of the Power System (L5) states.

	Eng_State	SuperTurbo_State	HSFW_State	MGU_State
Engine normal Run	1	-1	0	0
Engine normal Run	-1	1	0	0
Engine accel	0	1	-r	-1+r
Engine Braking	-1	0	r	1-r

The L5 power request for each L4 subsystem (Engine, SuperTurbo, HSFW, MGU) were calculated for each energy flow path using closed loop PI controllers with the potential to simplify using open loop controllers at feasible engine conditions. For example, during engine normal running PI controllers with intake manifold absolute pressure (IMAP) error as an input were used to calculate how much unnecessary high flow turbo energy could be harvested (turbo compounding) or how much power could be drawn from other system to assist the turbo during a transient event demanding more air flow.

L5 power limiting was defined based on each L4 subsystem hardware constraints. These power limits were used to constrain the L5 power request together with a PID anti-windup strategy. The final limited values were then dispatched to the individual L4 subsystems as target values to be reached.

L5 Controller Implementation

Implementation of the L5 controller was completed through multiple Simulink® / state flow models. The integrated system level model was then fast built into a dynamic linked library .dll file to be executed together with the physics-based L4 subsystem level plant models and controls in the DYNASTY simulation environment. Model update was through GIT version control which provided reliable tracking and sustained quality. Model calibrations were completed through the interface without having to manage calibration related .dll rebuilds.

L5 Controller Calibration for Concept Evaluation

Control parameters for baseline hardware constraints and controller stabilities were defined and calibrated first. Two different hardware configurations, coving a range of sizes, were set up and integrated with the L5 controller. The corresponding design of experiment (DOE) matrices, which reflected the differences in plants, were then tabulated with additional control calibration matrices for a full DOE run. The goal of the DOE run was to find optimal hardware and software configurations for the 19 work cycles reference in Figure 15. A total of 16 parameters were selected for the DOE to represent the storage level and energy transition criteria, and resulted in exploration of the trade-off between fuel consumption and transient capability. The DOE results showed that the winning parameter set provided fast energy recovery to take advantage of the braking opportunities, but was not too aggressive to inhibit upcoming transient assist capability. Of note is the HSFW energy and SOC as the power available is dependent on square of flywheel speed. Therefore, the calibration was biased to a higher percent SOC to give enough margin to support high levels of transient response power assisting.

Core Engine Performance Simulations

The major component of the off-road Power System is the core engine, and therefore significant effort was placed on improving the efficiency of the core engine. The critical building blocks toward improving the concept engine efficiency come from the following:

- Increased Peak Cylinder Pressure (PCP)
- Higher Compression Ratio (CR)
- Lower friction
- Improved combustion
- Improved breathing
- Optimized cooling
- Reduced aftertreatment restriction

Many of these same critical building blocks can also be found in the DOE SuperTruck II programs [7-11], but in this work they are tailored to the different needs and constraints of the off-road applications. An illustrative example of this is PCP, CR and engine power density. In the on-highway SuperTruck II programs the core engine's power density is not significantly increasing, and may even be decreasing, while here the power density needs to increase by 30% to match the larger 18L engine. This drives a need for more airflow, cylinder trapped mass, fuel energy, and therefore cylinder pressure. The power density limits the CR increase, and the degree of optimal combustion phasing possible, under the engine structural constraints. Preliminary scoping work in [16] helped to guide the current optimization of the combustion system under these constraints. The increase in specific load also challenges the desire and potential for friction reduction, regarding both tribological and parasitic aspects.

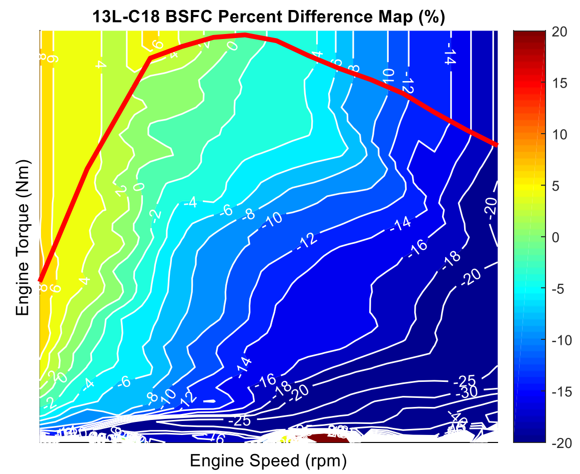

Figure 21. DYNASTY 1D engine simulations of the concept 13L engine efficiency percent difference from the C18 baseline.

Despite these challenges, significant improvements in engine efficiency, or brake specific fuel consumption (BSFC), were found and predicted by 1D engine cycle simulations in Figure 21. This is the condition with the concept 13L using a conventional single-stage turbocharger, and are comparisons between 13L simulations and 18L simulations. The greatest improvements (negative values) can be seen to occur at high speed and lower torque, but up to double digit percent improvements are predicted even along the lug curve (red line).

Heat Rejection and Thermal Barrier Coatings

A secondary, but significant, core engine benefit was found in the area of the off-road machine cooling system. Extending the analysis into the machine level starts to move outside the Power System paradigm but is worthwhile due to the direct linkage to core engine of the Power System. A byproduct of the increased core engine efficiency is a reduction in heat rejection and engine coolant system heat loading. Cascading this reduced heat rejection requirement downstream to the radiators, heat exchanges, cooling fans, and fan drives, a notable difference in cooling parasitic was found in Figure 22. This is an example of only one application cycle of the 745AT. The cooling parasitic requirement of slow/non-moving off-road machines without a free stream of cooling air is substantial. The 30-50% difference in Figure 22 translates to ~2.5% efficiency at the engine and Power System boundary. This analysis is for the engine-only heat rejection and the accounting for increased heat rejection from the hybrid elements, namely the HSFW and MGU systems, is expected to erode this ~2.5% efficiency benefit.

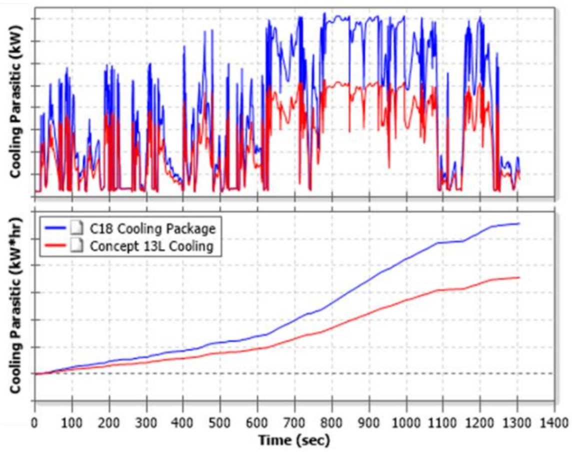

Figure 22. Concept 13L (engine-only Power System) cooling package parasitic reduction for 745AT cycle #5

Closely related to heat rejection is the topic of in-cylinder heat transfer and the reduction of which by thermal barrier coatings (TBC). There has been much renewed interest in TBCs since the recent work from Toyota Motor Corporation [23], where a "Temperature Swing" 1D heat conduction concept was presented. This work emphasized the importance of both low thermal conductivity and low volumetric heat capacity for coating properties. Continuing from this work Toyota outlined a porous anodized aluminum TBC called "SiRPA" [24] and showed heat flux reductions in metal and optical single cylinder diesel engines with coated pistons. Extended work in [25] emphasized the importance of TBC surface roughness, zone coating of pistons, and diesel engine cold-start benefits. General Motors Company and University Polytechnique Valencia in [26] found that permeable porosity brought a combination of experimental loss pathways that outweighed the theoretical heat loss benefits in a pre-mixed SI engine combustion. This work emphasized the need to seal a porous TBC from the cylinder constituents, and continued General Motors work with HRL [27] focused on the development of a novel sealed hollow nickel sphere TBC. Efficiency benefits of +2.7% on cold start and catalyst thermal management were found when using this to insulate diesel engine exhaust ports. In-cylinder application of this particular TBC is expected to provide ~2% efficiency gain.

An example of more conventional ceramic-based TBC research is from Volvo and Chalmers [28] on a light duty diesel piston. Using robust statistical analysis, the light-duty research found no significant efficiency benefit and found that the TBC surface roughness was a dominant factor deteriorating heat transfer and heat release rates. A final example of conventional TBC research is from the U.S. Army, Wisconsin-Madison and Stony Brook Universities [29] on a heavy-duty diesel piston. This research found similar deterioration with rough TBC surfaces but found up to ~4% indicated efficiency gains with polished TBC surfaces. It is clear that many factors about the TBC design, the combustion system design, and the operating conditions influence the resulting efficiency and heat transfer.

The present work simulated the impact of conventional ceramic based TBCs toward reduced heat transfer in increased efficiency through 3D CFD (CONVERGE) and 1D (DYNASTY) engine cycle simulation tools. Figure 23 is an example of the 3D CFD capability to predict local surface temperature ('bound_temp' legend) variation under different TBC properties and designs. The 3D CFD was used to help understand the finer details of the TBC parameters such as where to spatially place the TBC, how thick the TBC should be, and how rough or smooth it should be. It was also used to help validate the magnitude of predictions from the system level 1D engine cycle simulations.

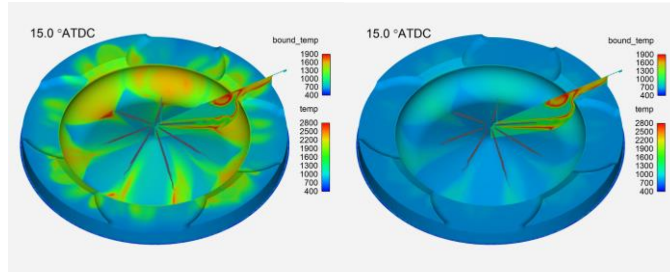

Figure 23. An example of 3D CFD simulations of TBC (left) and Steel (right) piston surface temperatures showing predictions of large local increases during flame/spray-wall interaction.

Figure 24 and Figure 25 present 1D engine simulation efficiency percent different maps over the engine speed and torque operation for a conventional ceramic-based supplier coating and the GM-HRL novel nickel sphere coating, respectively. These only show the impact of the coating as if they were applied to the final concept engine and are do not include any other engine parameter/calibration changes or efficiency technologies. Figure 26 plots the representative full load instantaneous surface temperatures for the TBC and baseline cases from the 1D simulations. In these figures the surfaces with TBC properties were the piston, cylinder head, exhaust port, intake and exhaust valve surfaces. Within each surface boundary the TBC was uniform without coating property spatial variation. No deterioration or assumption about how the TBC would change mixing-controlled combustion was applied.

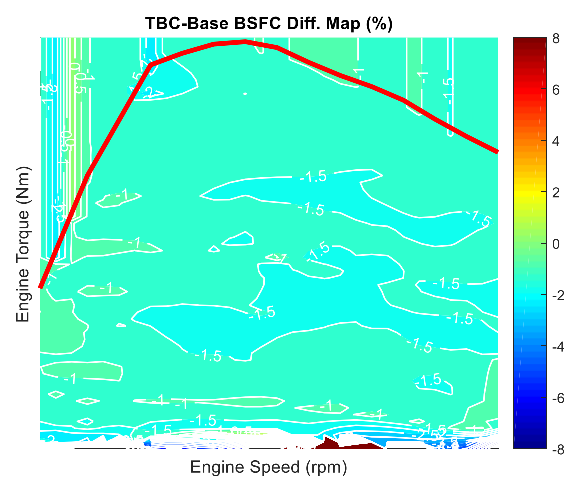

Figure 24. DYNASTY 1D engine simulations of the efficiency percent difference from the Supplier #2 TBC #2 applied to all surfaces except the cylinder liner and intake port.

The excellent thermophysical properties of the GM-HRL coating manifest themselves as up to 5% brake efficiency improvement (negative % differences). This is helpful for comparison and trend verification to the traditional ceramic-based TBC in Figure 24 where only up to 1.5% brake efficiency is predicted. Again, the prediction can be explained through the different “Temperature Swing” behaviors, a temporally varying reduction of convection ΔT, where larger temperature swings are clearly seen for the GM-HRL coating.

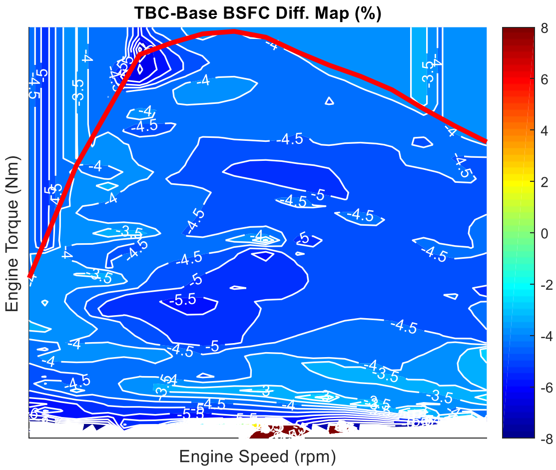

Figure 25. DYNASTY 1D engine simulations of the efficiency percent difference from the GM-HRL [27] TBC applied to all surfaces except the cylinder liner and intake port.

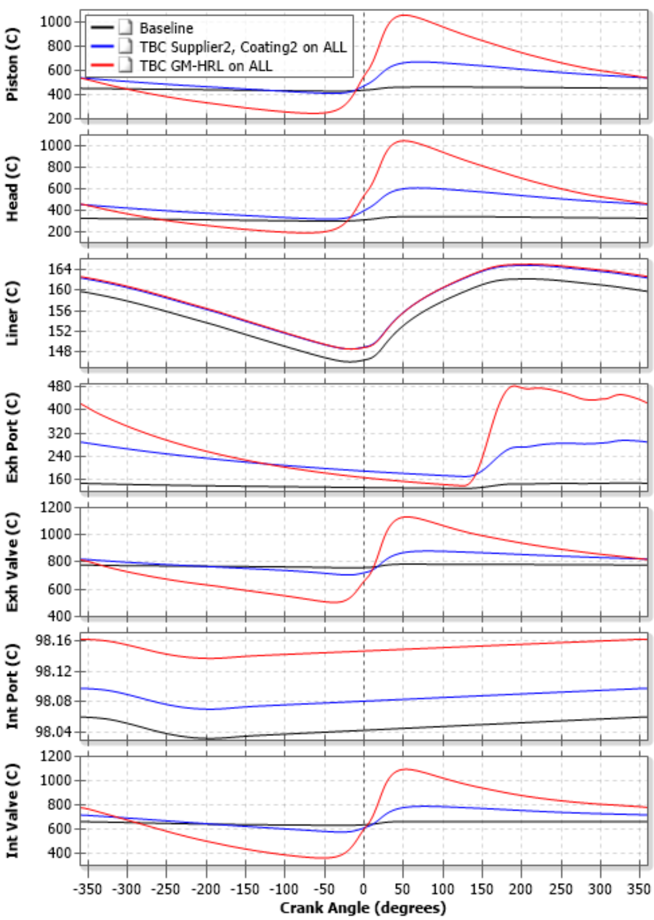

Figure 26. Full load in-cylinder component surface temperatures from the DYNASTY 1D engine simulations for the baseline and two TBCs applied to the piston, cylinder head, exhaust port, intake and exhaust valve surfaces. Individual surfaces were treated to be uniform without coating property spatial variation.

Validation of the efficiency improvement predictions by single cylinder testing in Figure 27 confirms the conventional ceramic-based TBC potential. Application of TBCs to in-cylinder surfaces will be included in the concept engine given that even ~1.5% efficiency improvement is significant and impactful.

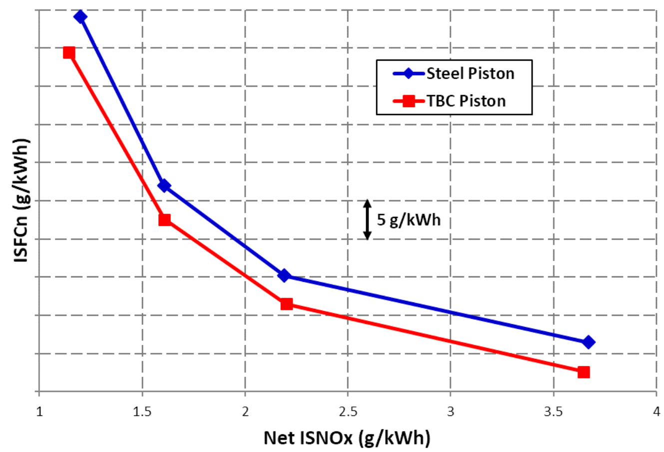

Figure 27. Heavy-duty single cylinder trade-off test data of indicated efficiency vs. NOx showing the potential of traditional ceramic based TBCs to improve efficiency.

SuperTurbo Turbocompounding

For this project, a mechanical transmission SuperTurbo is employed.

A high-speed planetary traction drive in combination with continuously variable transmission enables compounding or assisting as power moves between the turbine shaft and engine shaft (see Figure 29). During transient operation or acceleration conditions, the SuperTurbo is in supercharging mode which boosts the engine quickly and helps deliver power on-demand. At steady, higher-load operating conditions, SuperTurbo operates in turbo-compounding mode which transfers power from the turbine shaft to the engine shaft. At peak loads where the available exhaust energy is higher, more turbo-compounding can be done compared to lower loads.
Turbocompounding is traditionally accomplished with a dedicated power turbine downstream of the conventional turbocharger [17-19]. The SuperTurbo offers increased capability, modularity, and flexibility [19-22] with the ability to actively control the CVT ratio and not require a separate power turbine.

To increase the system efficiency, the SuperTurbo is sized and configured to run in a turbocompounding condition in the desired operating regions. This is achieved by changing the SuperTurbo CVT ratio and restricting the compressor/turbine speed. 17191922The 1D engine simulation data in Figure 28 highlights where the SuperTurbo turbocompounding is producing an efficiency benefit (negative values). It should be noted that the simulation predictions at very low load have high uncertainty. There are mid to full load regions of reduced efficiency, but these are at lower speeds that do not coincide with significant usage per the application histograms. In contrast, the high load regions of benefit were designed around the key application histograms. The trade-off between reduced aftertreatment restriction and EGR-driving capability can be better utilized for efficiency when turbocompounding is available. Therefore, future SuperTurbo calibration and turbine housing sizing will be completed as the project progresses towards physical demonstration with refined air system knowledge.

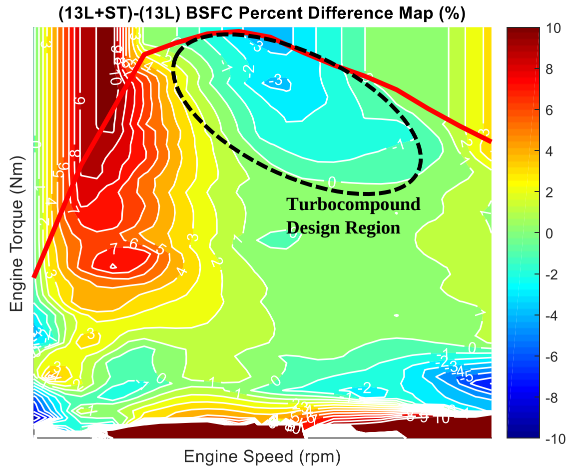

Figure 28. DYNASTY 1D engine simulations of the concept 13L with SuperTurbo engine efficiency percent difference from the concept 13L without SuperTurbo.

The SuperTurbo turbine is designed for higher efficiency versus a conventional turbocharger turbine, as the design is unconstrained by transient considerations as a result of the supercharging capability. This higher turbine efficiency adds to the engine fuel economy benefit in addition to aiding turbo-compounding. The transient response benefit also supports engine down-speeding, which is not evaluated in this project. The use of turbo-compound can also drive higher EGR flow rates, particularly at low load & low speed, due to increased back pressures.

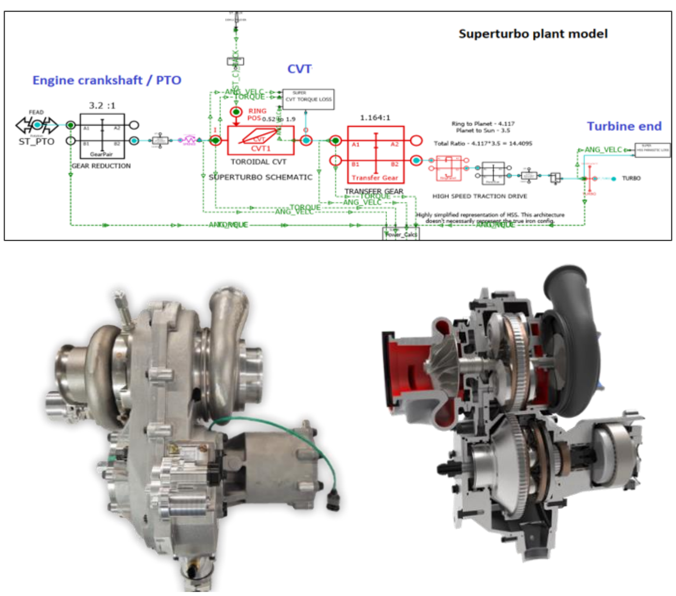

Figure 29. SuperTurbo drivetrain model & prototype images.

In summary, with SuperTurbo, control over boost, air flow rate & EGR flow rates enables tuning of the engine for lower emissions and higher efficiency compared to conventional turbo chargers. Specifically:

- Higher boost rates during accelerations improve transient response and help avoid rich air-fuel ratio combustion, thus reducing soot / smoke.
- Higher or optimized EGR flow rates enables lower NOx emissions.
- Application duty cycle fuel economy is improved through a combination of turbo-compounding and the extraction of waste heat exhaust energy, lean AFR transient operation, improved turbine efficiency, and optimized AFR & EGR level during calibration.

SuperTurbo Technologies Inc. has provided drivetrain specifications for the SuperTurbo CVT and traction drive. As mentioned, Caterpillar's in-house engine simulation software DYNASTY has capability for engine & machine modeling and has been used for evaluating the SuperTurbo benefits. The SuperTurbo drivetrain modeled in software is shown in Figure 29 along with the integration to the Power System model and controllers.

SuperTurbo Technologies Inc. also provided high efficiency turbine performance data, which has been converted to DYNASTY compatible turbine maps as shown in Figure 30. This map has been used in the simulations while adjusting the turbine area factors according to the engine flow requirements.

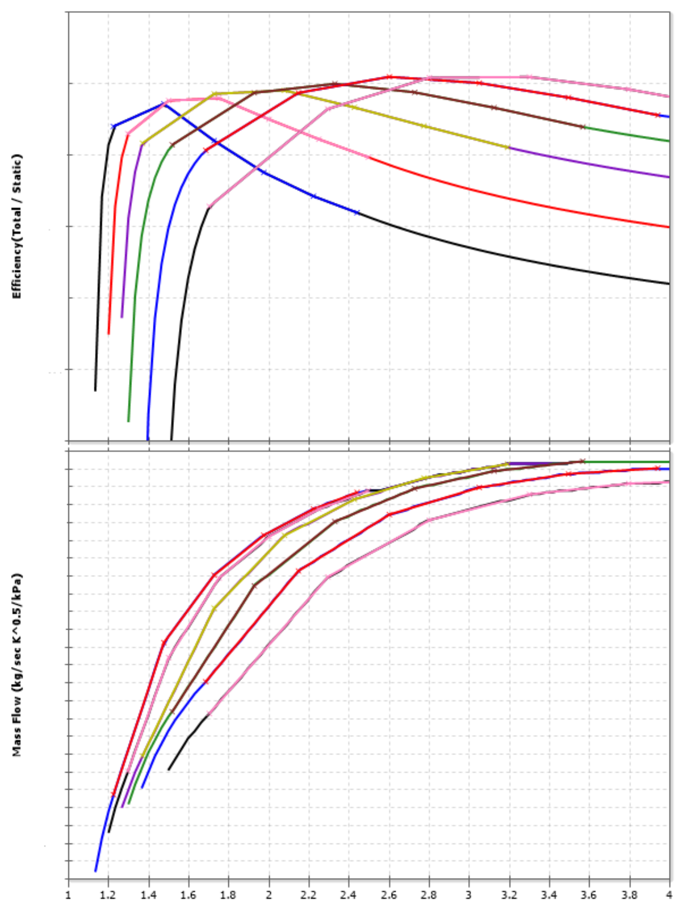

Figure 30. SuperTurbo turbine map.

The engine has been calibrated in steady state mode in the simulation software by optimizing for better Total Specific Fluid Consumption or TSFC (Fuel + Emission fluid) throughout the engine operating range of speed & load. Constraints in the optimizer and parameters swept for optimization are shown below. Output of the optimizer would give the level of Turbo-Compounding, EGR level, and SOI for a turbine area factor at a specific speed & load.

CONSTRAINTS	PARAMETER SWEEP
1. Turbine inlet temp	1. Level of Turbo-Compounding
2. PCP	2. SOI
3. Engine-out NOx > 3 g/kWh	3. EGR %
4. CVT in/out torque	4. Turbine area factor

Based on the application work cycle histograms of the 988K large wheel loader and 745AT articulated truck, a weighted TSFC parameter based on three lug torque points at different rpm has been evaluated to look at the TSFC benefits of SuperTurbo based on steady state optimized simulations. The plots in Figure 31 based on weighted TSFC benefits show that for both applications 988K & 745AT, weighted TSFC benefit is about 1.5 % - 2.5 % compared to a VGT turbo at steady state.

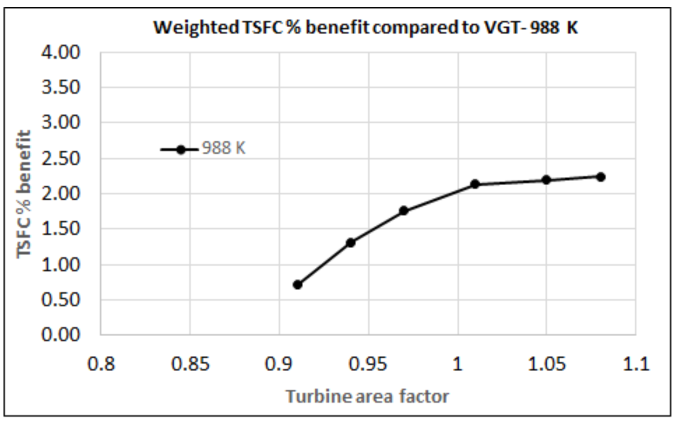

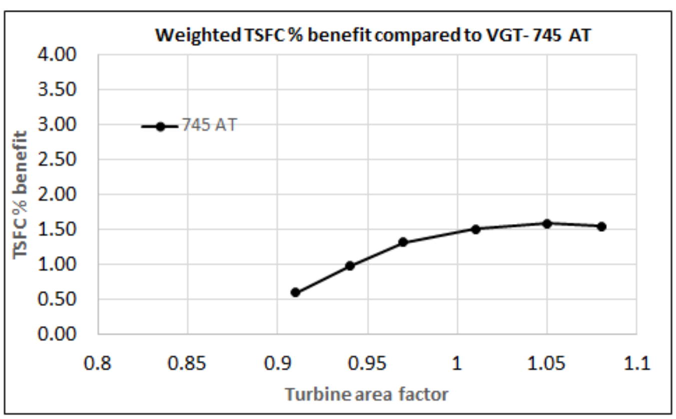

Figure 31. TSFC benefit from turbocompounding over a turbine area factor sweep.

The discussed benefit only shows the steady state benefit. Further relative benefits can be attained with duty cycle simulations because of improved transient response benefit with the resulting lower emissions.

Concept Core Engine Experimental Prototypes

The performance of the core engine concept has been tested on a phase 1 engine that includes the main core capabilities but not all the friction reduction improvements and overall design enhancements that will go into the eventual hybrid engine demonstration. This engine has enabled the verification of the performance improvements and provided input into the performance recipe down-selection on an adequate timeline to ensure that fully vetted decisions are made prior to the ultimate efficiency improvement demonstration. The test engine is based on a current Cat C13 engine with modifications to enable combustion and air system performance similar to the what the final Power System phase 2 concept engine will be, and is pictured in Figure 32.

Figure 32. Hybrid concept phase 1 engine early prototype.

Testing of the prototype engine started with motoring tests, correlation of soot measurements methodologies, and initial simulation validation tests. Good agreement was obtained between the friction mean effective pressure (FMEP) calculated from the motoring test versus the motoring FMEP from the friction model that is built into the phase 1 1D engine model despite the historically noisy character of this measurement, and adjustments were made to the model at high speed to improve agreement. As mentioned, this is the baseline friction level confirmation and model calibration prior to the friction improvements which will be made to the phase 2 concept engine. Soot correlation tests were completed so that the offset for microsoot measurements, which can be recorded at rapid intervals, could be correlated with the standard certification measurement of gravimetric filter weights and traditional filter blackening measurements at a variety of speeds, loads, and sooting conditions. This engine is being used to verify model performance of the turbocharger and combustion systems, and to choose optimized hardware for best performance. Although optimization of hardware is not completed, Figure 33 shows a comparison of the fuel consumption predicted by the simulation model vs. the fuel consumption realized in the test engine thus far during development testing. Much of the operating range is falling below 2% in agreement with the pre-hardware predictions, indicating that most of the improvement predicted above is being achieved in the prototype. At lower loads, the agreement gets worse as the friction reduction that is included in the simulation (of the final Power System concept engine) is not included in this prototype test becomes a larger factor in performance.

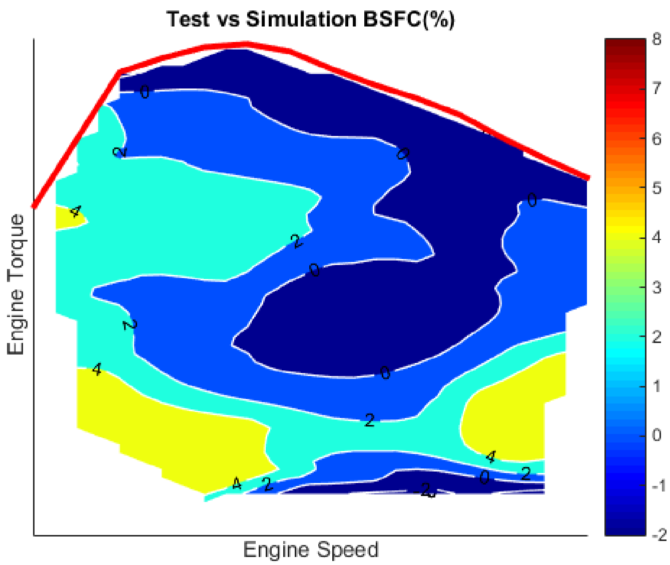

Figure 33. Prototype BSFC performance vs. simulation

Conclusions and Future Work

The concept definition phase of a multi-year off-road Power System project was researched through extensive simulation, experience, and the start of physical testing. Contributions from a mechanical hybrid subsystem, an electrical hybrid subsystem, engine start/stop, core engine technologies, turbocompounding, and heat rejection reduction combined to indicate confidence in the achievement of the project's efficiency improvement goal of 17 (+/-2) %. Table 2 lists the concept definition efficiency predictions by contributions from the individual Power System aspects.

Table 2. Current predictions of the Power System's high-level efficiency contributions over the baseline 18L engine Power System

7.2-10.6%	13L Concept engine
1.5-2.5%	SuperTurbo Turbo-compounding
1.5-2.0%	High-Speed Flywheel (HSFW) & 48V MGU
0.5-2.0%	Thermal Barrier Coatings (TBC)
2.0-4.0%	Start/stop implementation
2.0-3.0%	Reduced Cooling Parasitic
14.7-24.1%	Current Total

Transient Response Also Enables Engine Eff.

As well as the efficiency breakdown summary, the following conclusions were found:

- 30% engine downsizing brings very difficult transient load response requirements and hybrid devices (SuperTurbo, HSFW, MGU) with enough power can be used to offset base engine response deterioration.
- The mechanical CVT for the HSFW was found to be too immature for the current dynamic needs of fast power regeneration and assisting. Therefore, an electric drive CVT pathway was forced for realistic physical demonstration. Continued mechanical CVT development should not be completely abandoned though.
- Both mechanical and electrical energy pathways for the SuperTurbo were found to be possible with similar energy efficiency.
- The core engine efficiency predictions were verified at mostly below 2% error by testing of a preliminary prototype engine.

Due to the successful concept definition the project will progress into the hybrid Power System build and physical demonstration phases. As discussed, the physical demonstration will culminate with full system testing in a high-capability Power System test cell at Caterpillar's Technical Center.

References

1. Cat® 336E H Hybrid Excavator Press Release October 2012, https://www.cat.com/en_US/news/machine-press-releases/cat-sup-174-sup-336ehhydraulichybridexcavatordeliversnocompromis.html, accessed October 5, 2020.
2. Cat® D7E Dozer Press Release November 2014, https://www.cat.com/en_US/news/machine-press-releases/updated-cat-d7e-featuresadvancedtechnologytoboostproductivityand.html, accessed October 5, 2020.
3. Cat® D6 XE Electric Drive Dozer Press Release November 2018, https://www.cat.com/en_US/news/machine-press-releases/new-cat-d6-debuts-worlds-first-high-drive-electric-drive-dozer.html, accessed October 5, 2020.
4. Cat® 988K XE Electric Drive Wheel Loader Press Release August 2017, https://www.cat.com/en_US/news/machine-press-releases/new-electric-drive-cat-988kxe-wheel-loader-offers.html, accessed October 5, 2020.
5. University of Wisconsin-Madison, "Improving Efficiency of Off-Road Vehicles by Novel Integration of Electric Machines and Advanced Combustion Engines," U.S. Department of Energy FOA # DE-FOA-0002044, 2019.
6. Michigan Technical University, "Improved Efficiency of Off-Road Material Handling Equipment through Electrification," U.S. Department of Energy FOA # DE-FOA-0002044, 2019.
7. Dickson, J., Cummins Inc., and Damon, K., Peterbuilt Motors Company., "2020 Annual Merit Review Cummins/Peterbilt SuperTruck II," U.S. Department of Energy Vehicle Technologies Office 2020 Annual Merit Review and Peer Evaluation Meeting, June 1-4, 2020.
8. Villeneuve, D., and Girbach, J., Daimler Trucks North America., "Improving Transportation Efficiency Through Integrated Vehicle, Engine, and Powertrain Research -SuperTruck 2," U.S. Department of Energy Vehicle Technologies Office 2020 Annual Merit Review and Peer Evaluation Meeting, June 1-4, 2020.
9. Meijer, M., and Grover, B., PACCAR Inc., "Development and Demonstration of Advanced Engine and Vehicle Technologies for Class 8 Heavy-Duty Vehicle (SuperTruck II),"U.S. Department of Energy Vehicle Technologies Office 2020 Annual Merit Review and Peer Evaluation Meeting, June 1-4, 2020.

10. Amar, P., and Li, J., Volvo Group North America., "Volvo SuperTruck 2 Pathway to Cost Effective Commercialized Freight Efficiency," U.S. Department of Energy Vehicle Technologies Office 2020 Annual Merit Review and Peer Evaluation Meeting, June 1-4, 2020.
11. Zukouski, R., Cigler, J., Opperman, D., Navistar Inc., "Navistar SuperTruck II Development and Demonstration of a Fuel Efficient Class 8 Tractor & Trailer," U.S. Department of Energy Vehicle Technologies Office 2020 Annual Merit Review and Peer Evaluation Meeting, June 1-4, 2020.
12. Gibson, D., "A Flexible Fuel Injection Simulation," SAE Technical Paper 861567, 1986, doi:10.4271/861567.
13. Fluga, E., "Modeling of the Complete Vehicle Powertrain Using ENTERPRISE," SAE Technical Paper 931179, 1993, doi:10.4271/931179.
14. Williams, D., Koci, C., and Fiveland, S., "Compression Ignition 6-Stroke Cycle Investigations," SAE Int. J. Engines 7(2):656-672, 2014, doi:10.4271/2014-01-1246.
15. Xue, X. and Rutledge, J., "Potentials of Electrical Assist and Variable Geometry Turbocharging System for Heavy-Duty Diesel Engine Downsizing," SAE Technical Paper 2017-01-1035, 2017, https://doi.org/10.4271/2017-01-1035.
16. Koci, C., and Patyal, A., "Evaluation of Direct-Injection Burn Rates for Future Mixing-Controlled Combustion Engines," Presented at 28th Aachen Colloquium Automobile and Engine Technology, Aachen Germany, October 7-9, 2019.
17. Holtman, R., "Testing of a Low Specific Fuel Consumption Turbocompound Engine," SAE Technical Paper 870300, 1987, https://doi.org/10.4271/870300.
18. Brands, M., Werner, J., Hoehne, J., and Kramer, S., "Vehicle Testing of Cummins Turbocompound Diesel Engine," SAE Technical Paper 810073, 1981, https://doi.org/10.4271/810073.
19. Jääskeläinen, H., and Majewski, W., "Turbocompounding," Dieselnet Technology Guide, Waste Heat Recovery, https://dieselnet.com/tech/engine_whr_turbocompound.php, accessed October 9, 2020.
20. Chadwell, C. and Walls, M., "Analysis of a SuperTurbocharged Downsized Engine Using 1-D CFD Simulation," SAE Technical Paper 2010-01-1231, 2010, https://doi.org/10.4271/2010-01-1231.
21. Suelter, B., Itou, T., Waldron, T., and Brin, J., "Optimizing Steady State Diesel Efficiency and Emissions Using a SuperTurboTM on an Isuzu 7.8L Engine," SAE Technical Paper 2019-01-0318, 2019, https://doi.org/10.4271/2019-01-0318.
22. Neely, G., Sharp, C., and Rao, S., "CARB Low NOx Stage 3 Program - Modified Engine Calibration and Hardware Evaluations," SAE Technical Paper 2020-01-0318, 2020, https://doi.org/10.4271/2020-01-0318.
23. Kosaka, H., Wakisaka, Y., Nomura, Y., Hotta, Y. et al., "Concept of "Temperature Swing Heat Insulation" in Combustion Chamber Walls, and Appropriate Thermo-Physical Properties for Heat Insulation Coat," SAE Int. J. Engines 6(1):142-149, 2013, https://doi.org/10.4271/2013-01-0274.
24. Wakisaka, Y., Inayoshi, M., Fukui, K., Kosaka, H. et al., "Reduction of Heat Loss and Improvement of Thermal Efficiency by Application of "Temperature Swing" Insulation to Direct-Injection Diesel Engines," SAE Int. J. Engines 9(3):1449-1459, 2016, https://doi.org/10.4271/2016-01-0661.
25. Kawaguchi, A., Wakisaka, Y., Nishikawa, N., Hidemasa Kosakaet, H., et al. "Thermo-Swing Insulation to Reduce Heat Loss from the Combustion Chamber Wall of a Diesel Engine" International Journal of Engine Research 20, no. 7, September 2019: 805–16. https://doi.org/10.1177/1468087419852013.
26. Andruskiewicz, P., Najt, P., Durrett, R., and Payri, R., "Assessing the Capability of Conventional In-Cylinder Insulation Materials in Achieving Temperature Swing Engine Performance Benefits" International Journal of Engine Research 19, no. 6, August 2018: 599–612. https://doi.org/10.1177/1468087417729254.
27. Schaedler, T., Hughes Research Laboratories., "Temperature Following Thermal Barrier Coatings for High Efficiency Engines," U.S. Department of Energy Vehicle Technologies Office 2020 Annual Merit Review and Peer Evaluation Meeting, June 1-4, 2020.
28. Somhorst, J., Oevermann, M., Bovo, M., and Denbratt, I., "Evaluation of Thermal Barrier Coatings and Surface Roughness in a Single-Cylinder Light-Duty Diesel Engine" International Journal of Engine Research, October 2019, https://doi.org/10.1177/1468087419875837.
29. Gingrich, E., Tess, M., Korivi, V., Schihl, P., et al. "The Impact of Piston Thermal Barrier Coating Roughness on High-Load Diesel Operation." International Journal of Engine Research, December 2019, https://doi.org/10.1177/1468087419893487.

Contact Information

Chad P. Koci: (309) 675-6747

Koci_Chad@cat.com

Acknowledgments

This research was conducted with funding from the U.S. Department of Energy, Office of Energy Efficiency and Renewable Energy, Vehicle Technologies Office, under the award DE-EE0008476. The authors would specifically like to acknowledge Department of Energy managers David Ollett and Michael Weismiller for their continued support and guidance. In addition, the authors would like to thank the numerous Caterpillar engineering and technical contributors at the Mossville Technical Center and engine business units, as without this support the program could not exist. The technical and management staff at SuperTurbo Technologies Inc. is also greatly acknowledged for their critical support and expertise on the technology integration of the SuperTurbo.

Definitions/Abbreviations

1D	One dimensional
3D	Three dimensional
AFR	Air Fuel Ratio
AT	Articulated truck
BSFC	Brake specific fuel consumption
CAD	Computer aided design
CFD	Computational fluid dynamics
CR	Compression ratio
CSLA	Constant speed load acceptance

CVT	Continuously variable transmission
DOE	Design of experiment
EGR	Exhaust gas recirculation
FEAD	Front end accessory drive
FMEP	Friction mean effective pressure
HEX	Hydraulic excavator
HPC	High Performance Computing
HSFW	High-speed flywheel
IMAP	Intake manifold absolute pressure
L4	Controller level for the components and subsystems of the Power System
L5	Controller level of the Power System
LWL	Large wheel loader
MGU	Motor-generator unit
PCP	Peak cylinder pressure
PI	Proportional integral controller
PID	Proportional integral derivative controller
R&D	Research and development
SI	Spark ignition
SOC	State of charge
SOI	Start of injection
ST	SuperTurbo
TBC	Thermal barrier coating
TC	Torque converter
TCO	Total cost of ownership
TSFC	Total specific fluid consumption
VGT	Variable geometry turbocharger